Available online at www.sciencedirect.com
SCIENCE DIRECT®
Journal of Nuclear Materials 352 (2006) 224–232
journal of nuclear materials
www.elsevier.com/locate/jnucmat

Immobilization of tetravalent actinides in phosphate ceramics

O. Terra [a,b], N. Dacheux [a,*], F. Audubert [b], R. Podor [c]

[a] Groupe de Radiochimie, IPN Orsay, Bât. 100, Université, Paris-Sud-11, 91406 Orsay, France
[b] CEA Cadarache, DEN/DEC/SPUA/LTEC, Bât. 307, 13108 Saint Paul Lez Durance, France
[c] LCSM (CNRS UMR 7555), Université H. Poincaré-Nancy I, BP, 239, 54506 Vandœuvre lès Nancy, France

Abstract

Three phosphate-based ceramics were studied for the immobilization of tri- and tetravalent actinides: britholite $Ca_9Nd_{1-x}An^{IV}_x(PO_4)_{5-x}(SiO_4)_{1+x}F_2$, monazite/brabantite $Ln^{III}_{1-2x}Ca_xAn^{IV}_xPO_4$ and thorium phosphate diphosphate $\beta - Th_{4-x}An^{IV}_x(PO_4)_4P_2O_7$ (β-TPD). For each material, the incorporation of thorium and uranium (IV) was examined through dry chemistry routes, using mechanical grinding of the initial mixtures then heating at high temperature (1373–1673 K). The quantitative incorporation of thorium in the britholite structure was obtained up to 20 wt% through the coupled substitution $(Nd^{3+},\ PO_4^{3-}) \Longleftrightarrow (Th^{4+},\ SiO_4^{4-})$. On the contrary, the incorporation of uranium was limited to 5–8 wt% and always led to a two-phase system composed by U-britholite and CaU_2O_{5+y}. The incorporation of Th and U(IV) was also examined in both matrices, β-TPD and monazite/brabantite solid solutions. Homogeneous and single phase samples of β-TUPD and (Th,U)-monazite/brabantite solid solutions were obtained using successive cycles of mechanical grinding/calcination. The three matrices were prepared in the pellet form then leached in 10^{-1} M or 10^{-4} M HNO_3 at 363 K. The very low normalized dissolution rates confirmed the good resistance of the materials to aqueous alteration. Moreover, in over-saturation conditions, the formation of neoformed phases onto the surface of the pellets was evidenced for several sintered samples.

PACS: 28.41.Kw; 81.20.Ev; 81.05.−t

1. Introduction

Several phosphates matrices such as britholite, monazite/brabantite and thorium phosphate diphosphate (β-TPD) were already proposed for the immobilization of radwaste of high activity and long-life radionuclides.

Nd-britholite ($Ca_9Nd(PO_4)_5(SiO_4)F_2$) was first prepared by Boyer et al. [1] in the field of the immobilization of trivalent actinides (Am, Cm) simulated by Nd^{3+}. This compound belongs to the apatite family and crystallizes in a hexagonal system ($P6_3/m$). In this work, the incorporation of tetravalent actinides was realized considering the coupled substitution $(Nd^{3+},\ PO_4^{3-}) \Longleftrightarrow (Th^{4+},\ SiO_4^{4-})$ leading to $Ca_9Nd_{1-x}An^{IV}_x(PO_4)_{5-x}(SiO_4)_{1+x}F_2$ samples with a weight loading of 10 wt% (which corresponds to a x value equal to 0.5 in the actinides-bearing samples).

* Corresponding author. Tel.: +33 1 69 15 73 46; fax: +33 1 69 15 71 50.
E-mail address: dacheux@ipno.in2p3.fr (N. Dacheux).

0022-3115/$ - see front matter © 2006 Elsevier B.V. All rights reserved.
doi:10.1016/j.jnucmat.2006.02.058

Both monazite $Ln^{III}PO_4$ (Ln = La–Gd) [2] and brabantite $Ca_{0.5}An^{IV}_{0.5}PO_4$ (An = Th, U, Np, Pu) [3,4] samples crystallize in a monoclinic system (space group $P2_1/n$). Podor et al. showed the existence of solid solutions between $LaPO_4$ and $Ca_{0.5}U_{0.5}PO_4$ or $Ca_{0.5}Th_{0.5}PO_4$ [5,6]. In this work, the elaboration of samples containing simultaneously trivalent lanthanides and tetravalent actinides (Th, U), i.e. $Ln^{III}_{1-2x}Ca_xAn^{IV}_xPO_4$, was developed.

Finally, the thorium phosphate diphosphate ($\beta Th_4(PO_4)_4P_2O_7$: β-TPD, orthorhombic system, space group *Pbcm*) [7] is especially dedicated to the immobilization of tetravalent actinides by substitution of thorium by other cations (U(IV), Pu(IV), Np(IV)) [8,9]. In this work, only tetravalent uranium was considered.

For each material, the incorporation of Th, U(IV) or Ce(IV) was studied through dry chemistry routes involving mechanical grinding to improve the homogeneity and the reactivity of the initial powders. The mixtures were thus heated at high temperature ($1373\ K \leqslant T \leqslant 1673\ K$) then extensively characterized using several techniques (XRD, SEM, EPMA, etc.). Dense pellets were prepared and finally leached in several media in order to evaluate their behavior during leaching tests.

2. Experimental

2.1. Characterization of the samples

Mechanical grindings of the powders were realized in a RETSCH MM200 apparatus with zirconium oxide balls and container. The X-ray powder diffraction (XRD) patterns were collected with a Bruker AXS D8 Advance diffractometer system using Cu K_α rays ($\lambda = 1.5418$ Å). TGA and DTA experiments were performed with a Setaram TG 92-16 apparatus. The electron probe microanalyses (EPMA) were carried out using a Cameca SX 50 or SX 100 apparatus using several calibration standards (topaz $Al_2SiO_4F_2$, orthose $KAlSi_3O_8$, monazites $LaPO_4$ and $NdPO_4$, wollastonite Ca_2SiO_4, thoria ThO_2 and uranium oxide $UO_{2.12}$). Scanning electron micrographs (SEM) were recorded with a Hitachi S2500 scanning electron microscope.

2.2. Sintering procedure

All the pellets were prepared through a two-steps procedure involving an uniaxial pressing at room temperature (100–200 MPa) then a heat treatment at high temperature. The dilatometric experiments were performed with a TMA 92-18 apparatus from Setaram, working in argon atmosphere. The relative density of the sintered samples was evaluated using water pycnometry after immersion and outgassing of the sample in the fluid (leading to the determination of the close porosity) while the determination of the dimensions of the pellets led to the geometrical relative densities.

2.3. Leaching tests procedure

The leaching tests were performed in PTFE vessels at 363 K. The concentrations of the cations released in the leachate were determined by inductively coupled plasma – mass spectroscopy (ICP-MS) for Nd, Th and U. The normalized dissolution rate R_L (g m^{-2} d^{-1}) was deduced from the following equation:

$$R_L(i) = \frac{dN_L(i)}{dt} = \frac{d}{dt}\left(\frac{C_i \times V \times M_i}{x_i \times S}\right), \quad (1)$$

where C_i represents the concentration of the measured element (Nd, Th, U), V the volume of the leachate, x_i the mass ratio of the element i in the solid and S the effective surface area of the pellet (determined by the BET method using N_2 adsorption).

3. Syntheses and characterizations of the powders

In order to simulate the further incorporation of plutonium from $^{238}PuO_2$ in the three matrices (study of their resistance to radiation damage), this study was focused on dry chemical processes involving ThO_2 or UO_2 as initial reagents. The homogeneity of the samples was improved by using successive steps of mechanical grinding/heating treatment.

3.1. Synthesis of britholites

The synthesis of britholite is based on some results reported by Boyer et al. [10] who prepared Nd-britholite ($Ca_9Nd(PO_4)_5(SiO_4)F_2$) samples by using a manual grinding of the initial mixture then its calcination at 1673 K for 6 h. In this work, the incorporation of thorium and uranium was examined using a mechanical grinding of a mixture containing $Ca_2P_2O_7$, CaF_2, CaO, Nd_2O_3, AnO_2 (An = Th or U) and SiO_2 then a heat treatment at 1673 K for 6 h under inert atmosphere (argon) to prevent any oxidation of uranium during the synthesis [11].

The incorporation of thorium in the structure was observed above 1373 K. The calcination at 1673 K led to the preparation of several homogeneous samples of (Nd,Th)-britholites $Ca_9Nd_{1-x}Th_x(PO_4)_{5-x}(SiO_4)_{1+x}F_2$ ($0 \leqslant x \leqslant 1$) exhibiting the expected stoichiometry. The EPMA experiments revealed the good substitution of neodymium by thorium and of phosphate by silicate groups. The linear increase of the refined unit cell parameters a and c when increasing the x value from 0 to 1 (i.e. $a(\text{Å}) = (9.4012 \pm 0.0006) + (0.019 \pm 0.001) \times x$ and $c(\text{Å}) = (6.9025 \pm 0.0007) + (0.015 \pm 0.001) \times x$) confirmed the formation of solid solutions between $Ca_9Nd(PO_4)_5(SiO_4)F_2$ and $Ca_9Th(PO_4)_4(SiO_4)_2F_2$ [12] which follow the Vegard's law.

The incorporation of uranium in the britholite structure was associated to the formation of intermediates like $CaUO_4$ and fluorapatite leading, after heating at 1673 K, to polyphase samples (Fig. 1) composed by (Nd,U)-britholite (with an uranium weight loading of 3–5 wt% instead of 10 wt% expected) and CaU_2O_{5+y} [12]. The incorporation of uranium in the britholite structure was increased up to 8–9 wt% by pressing the reactive mixture into pellets prior to perform the final calcination at 1673 K. In these conditions, the presence of CaU_2O_{5+y} was only observed onto the surface of the pellet.

3.2. Synthesis of brabantites and monazite/brabantite solid solutions

The preparation of monazites or brabantites was already reported in literature. Hikichi et al. [13] prepared $LnPO_4$ monazites using dry chemistry methods by mixing Ln_2O_3 with $(NH_4)_2(HPO_4)$ then firing at 1273 K, while Tabuteau et al. [4] synthesized brabantites of formula $Ca_{0.5}Np_{0.5-x}Pu_xPO_4$ ($x = 0$ and $x = 0.15$) at 1473 K from a mixture of NpO_2, PuO_2, $CaCO_3$ and $(NH_4)_2(HPO_4)$.

In this work, all the syntheses were based on the mechanical grinding of $Ca(HPO_4) \cdot 2\ H_2O$ (or CaO), $(NH_4)(H_2PO_4)$ and AnO_2 (An = Th or U) followed by a heating treatment ($T = 1473$ K, 10 h, argon). From XRD, the formation of brabantites $Ca_{0.5}Th_{0.5}PO_4$ and $Ca_{0.5}U_{0.5}PO_4$ occurred above 1023 and 1173 K, respectively. Well crystallized and single phase samples were prepared above 1373 K [14].

The preparation of (Th,U)-brabantites ($Ca_{0.5}Th_{0.5-y}U_yPO_4$ with $0 \leqslant y \leqslant 0.5$) was also examined considering several cycles of mechanical grinding (15 min, 30 Hz) and calcination (10 h, $T = 1473$ K, argon). For all the y-values considered, the XRD patterns revealed the preparation of single phase compounds. The linear decrease of a, b, c parameters and V, and the linear increase of β when increasing the y-value (V (Å^3) $= (289.35 \pm 0.05) - (12.7 \pm 0.2) \times y$) appeared in good agreement with the progressive replacement of thorium by uranium (IV) leading to the formation of $Ca_{0.5}Th_{0.5-y}U_yPO_4$ solid solutions. That was also confirmed by EPMA and μ-Raman experiments. On this basis, several compounds of the general formula $La^{III}_{1-2x}Ca_xTh_{x-y}U_yPO_4$ ($0 \leqslant x \leqslant 0.5$ and $y = x/5$) were also prepared through the same method [14].

3.3. Synthesis of β-TUPD solid solutions

Samples of β-TPD and associated solid solutions containing large amounts of tetravalent uranium, neptunium and plutonium were already prepared using wet chemical processes [7–9]. One of the main

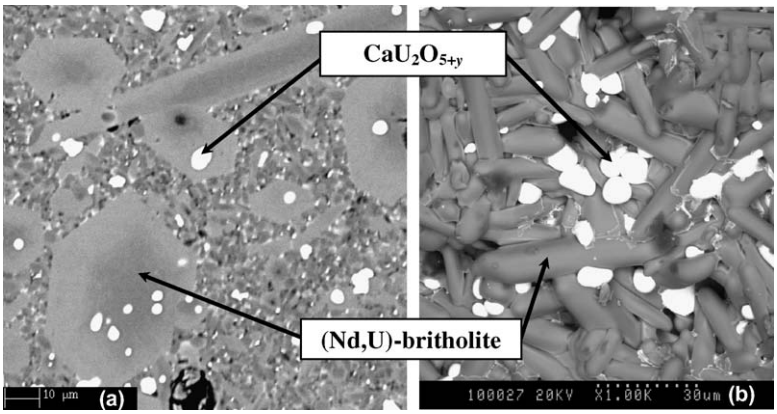

Fig. 1. SEM observations of (Nd,U)-britholite sample in BSE mode: core and polished surface (a) and raw surface (b).

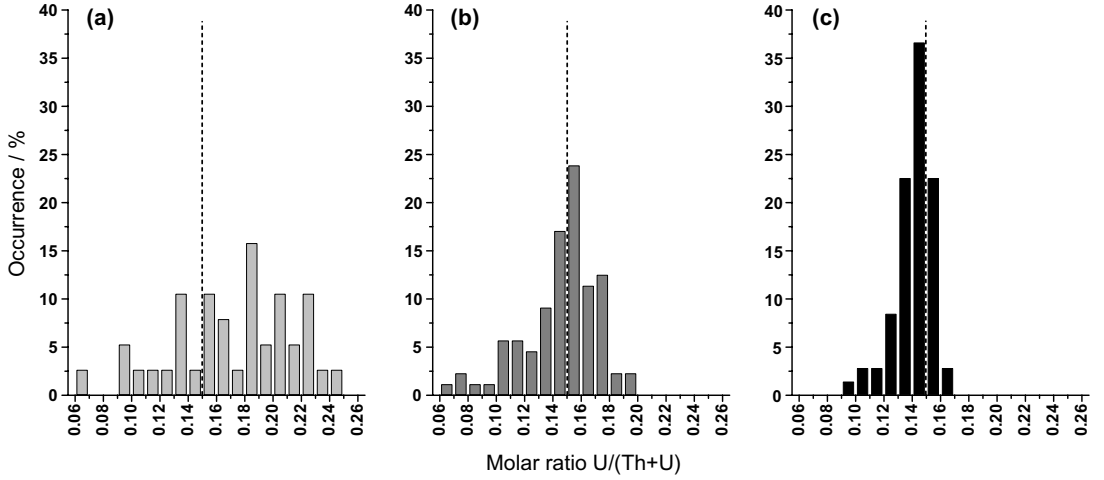

Fig. 2. Statistical variations of the U/(U + Th) molar ratio for β-TUPD samples: after one (a), two (b) and three (c) grinding/calcination cycles. The expected value is represented by a vertical dash line.

advantages of this chemical way of synthesis results from the homogeneity of the final samples prepared.

In this work, the incorporation of tetravalent uranium in the β-TPD structure was examined through dry chemistry method from a mixture of thorium phosphate hydrogenphosphate hydrate (TPHPH, $Th_2(PO_4)_2(HPO_4)\cdot H_2O$), UO_2 and α-ThP_2O_7 using successive mechanical grinding/calcination cycles (15 min, 30 Hz/$T = 1473$ K, 10 h, argon). The formation of such solid solutions was confirmed from XRD above 1123 K. Nevertheless, EPMA experiments showed that the compound remained rather heterogeneous with the presence of residual reagents at the micrometric scale after the first cycle (Fig. 2(a)). On the contrary, β-TUPD samples were single phase after the second cycle of grinding/calcination, even though a large dispersion of the mole ratio U/(Th + U) was observed (Fig. 2(b)), while the (Th + U)/PO_4 stoichiometry remained equal to 2/3. Finally, the distribution of tetravalent cations in the structure was significantly improved after the third cycle (Fig. 2(c)). Correlatively, the unit cell parameters and μ-Raman spectra were found to be in good agreement with that already reported in literature for β-TUPD solid solutions prepared from wet chemical processes [8,15].

4. Sintering

4.1. Preparation of (Nd,Th)-britholite pellets

The sintering of (Nd,Th)-britholite was realized from ground powdered $Ca_9Nd_{0.5}Th_{0.5}(PO_4)_{4.5}(SiO_4)_{1.5}F_2$ ($SA = 5\ m^2\ g^{-1}$) after initial compaction. The dilatometric curve (Fig. 3(a)) showed that the sintering process began near to 1273 K, with a maximum densification rate at 1553 K and was finished above 1673 K leading to an experimental relative density of (95 ± 1)%. The geometrical relative density reached only 80% after heating at 1573 K for 6 h, then increased up to 94–95% after heating for 6 h at 1673 K (Table 1). In these conditions, the sintering process appeared to be efficient with an increase of the grain size (2–20 μm: Fig. 4(a)). Nevertheless, the core of the samples exhibited a rather significant remaining close porosity (Fig. 4(b)).

4.2. Preparation of monazite/brabantites solid solutions pellets

Two kinds of experiments were considered to get densified samples of brabantites: the first one consisted in the same procedure than for (Nd,Th)-britholites while the second one was based on a reactive sintering.

The first kind of experiments was performed on $Ca_{0.5}Th_{0.5}PO_4$ brabantites initially ground to increase the specific surface area from 1 to 3–5 $m^2\ g^{-1}$, then pressed at 100–200 MPa. From dilatometric experiments (Fig. 3(b)), the densification began near to 1273 K and reached a maximum rate at about 1573–1623 K, the sintering being achieved at 1673 K. After this calcination treatment, the geometrical relative density of the pellet reached 93% of the calculated value. The optimal temperature of

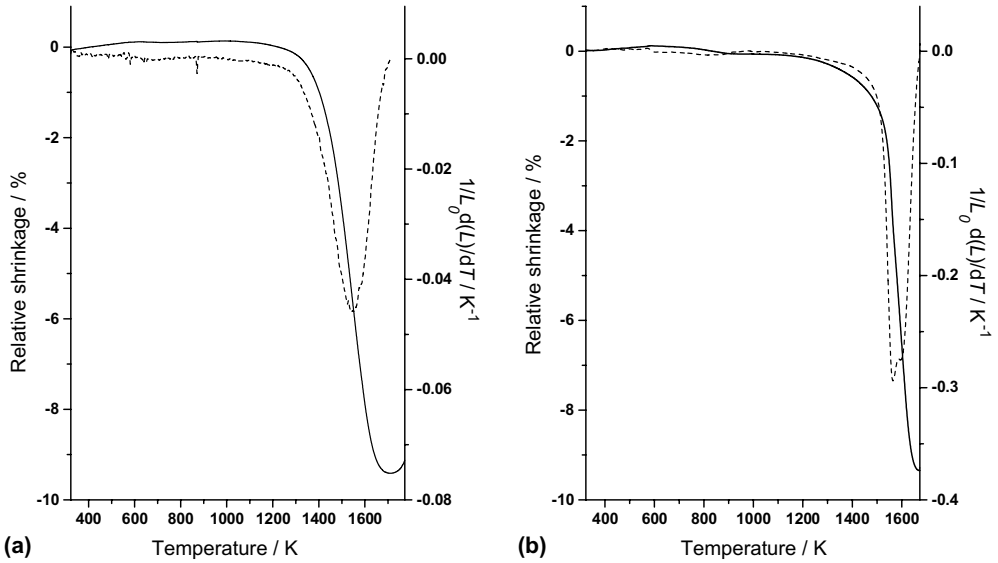

Fig. 3. Dilatometric curves of (Nd,Th)-britholite (a) and $Ca_{0.5}Th_{0.5}PO_4$ (b) versus temperature: relative linear shrinkage (main line) and derivative plot (dash line).

Table 1
Geometrical relative density and associated open and close porosity of (Nd,Th)-britholite pellets versus the heat temperature and the holding time

Temperature (K)	Holding time (h)	Geometrical relative density (%)	Open porosity (%)	Close porosity (%)
1573	6	78–80	6–7	14–15
1673	1	84	4	12
1673	3	84	9	7
1673	6	94–95	3	2–3

sintering of $Ca_{0.5}Th_{0.5}PO_4$ ($T = 1573$ K) appeared lower than that reported for $LaPO_4$ ($1673\ K \leqslant T \leqslant 1723$ K) [16]. The isotherm study developed at this temperature showed that the pellets fired for 6 h remained porous and badly densified ($d_{geom.}/d_{calc.} = 70–80\%$).

On the basis of these first observations, the reactive sintering of $Ca_{0.5}Th_{0.5}PO_4$ was developed from a ground mixture of $Ca(HPO_4) \cdot 2\,H_2O$, ThO_2 and $(NH_4)(H_2PO_4)$ ($SA = 2.9\ m^2\ g^{-1}$). The mixture was first heated at 1073–1173 K for 6 h then mechanically ground (20 Hz, 15 min), pressed at 100–200 MPa then finally fired for 6 h at several temperatures ranging from 1473 to 1673 K. The geometrical relative density reached 86% of the calculated

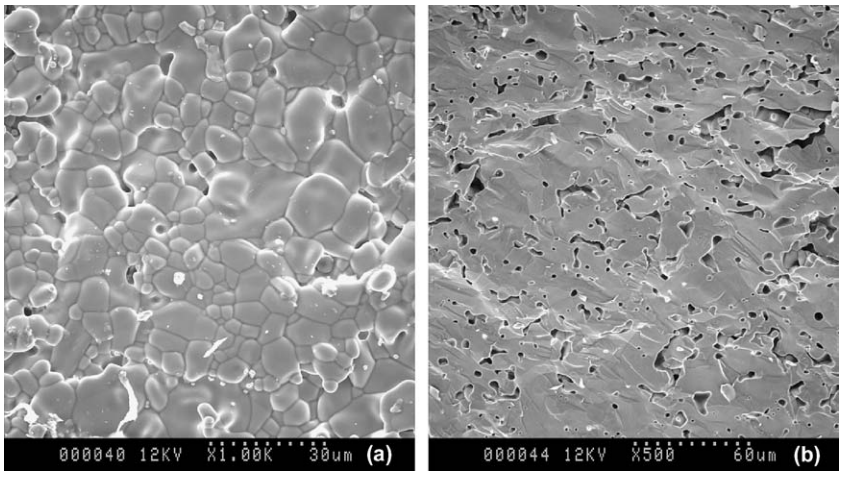

Fig. 4. SEM observations of sintered (Nd,Th)-britholite heated at 1673 K for 6 h: surface (a), core (b).

Table 2
EPMA results of $Ca_{0.5}Th_{0.5}PO_4$ pellets fired at 1573 K for 6 h and β-TUPD pellets calcinated at 1523 K for 10 h (both using reactive sintering)

	$Ca_{0.5}Th_{0.5}PO_4$		β-$Th_{3.4}U_{0.6}(PO_4)_4P_2O_7$	
	Calc.	Exp.	Calc.	Exp.
Weight percent				
O	27.7	27.9 ± 0.1	24.8	24.9 ± 0.1
P	13.4	13.4 ± 0.1	12.5	12.7 ± 0.1
Ca	8.7	8.9 ± 0.1	–	–
Th	50.2	49.8 ± 0.4	56.3	56.5 ± 0.8
U	–	–	6.4	5.9 ± 0.4
Molar ratio				
(Th + U)/Ca	1	0.96 ± 0.02	–	–
U/(Th + U)	–	–	0.100	0.093 ± 0.007
P/(Ca + Th + U)	1	0.99 ± 0.01	–	–
(Th + U)/P	–	–	0.667	0.65 ± 0.01

density at 1473 K and increased up to 90–95% after heating at 1573 K (open porosity: 1–5%; close porosity: 4–5%). The observation of the pellets by SEM revealed a good densification while the EPMA experiments showed a good agreement between the determined chemical composition with that expected (Table 2).

4.3. Sintering of β-TUPD solid solutions

For the same reasons than for monazite/brabantite samples, the sintering of β-$Th_{3.4}U_{0.6}(PO_4)_4P_2O_7$ was examined through two kinds of reactive sintering procedures: the first one involved an initial mixture of TPHPH, UO_2 and α-ThP_2O_7 (SA = 5 $m^2\ g^{-1}$) while the second one started from a mixture of TPHPH and β-TUPD.

The dilatometric study revealed a linear relative shrinkage of −1.9% between 423 and 723 K correlatively to the full dehydration of TPHPH then to the condensation of hydrogenphosphate group into diphosphate entities. Above 1073 K, an additional relative linear shrinkage of −2.7% was associated to the phase transition of α-TUPD into β-TUPD [17]. Finally, the sintering of β-TUPD solid solutions occurred between 1323 and 1523 K, which appeared consistent with literature [17]. At this later temperature, the geometrical relative density of the final pellet reached 93%.

When using a ground mixture of TPHPH and β-TUPD, the geometrical relative density reached 90-91% after heating at 1523 K for 10 h. Consequently, the small open porosity expected (1–2%) was confirmed by SEM while the EPMA experiments revealed an accurate final composition of the samples (Table 2). For the three materials, the optimal conditions of sintering are summarized in Table 3.

5. Leaching tests

The chemical durability of the three matrices was examined in several acidic media considering two kinds of leaching tests (static conditions with a low renewal of the leachate and dynamic conditions with a high and continuous renewal of the solution of 1 ml h^{-1}).

5.1. Leaching of sintered britholites samples

The leaching of (Nd, Th)-britholites and (Nd, U)-britholites in 10^{-4} M HNO_3 at 363 K revealed a significant release of Th, U and Nd during the first

Table 3
Optimal conditions of sintering considered for the three phosphate based matrices

Material composition	Conditions of preparation of initial powders	Sintering conditions		$d_{geom.}/d_{calc.}$ (%)
		T (K)	t (h)	
$Ca_9Nd_{0.5}Th_{0.5}(PO_4)_{4.5}(SiO_4)_{1.5}F_2$	Mechanical grinding/Heating: 1673 K – 6 h	1673	6	94–95
$Ca_{0.5}Th_{0.5}PO_4$	Mechanical grinding/Heating: 1173 K – 6 h	1573	6	90–95
β-$Th_{3.4}U_{0.6}(PO_4)_4P_2O_7$	Mechanical grinding	1523	10	93

20 days of leaching time leading to normalized dissolution rates $R_L(Nd)$ and $R_L(Th)$ equal to $(4.0 \pm 0.8) \times 10^{-4}$ and $(1.3 \pm 0.5) \times 10^{-4}$ g m^{-2} d^{-1}, respectively. Then, the normalized leaching decreased strongly showing the precipitation of secondary phases onto the surface of the pellets.

Both values appeared lower than that reported when leaching Nd-britholite ($R_L(Ca) = (3.0 \pm 0.5) \times 10^{-1}$ g m^{-2} d^{-1}) [11,18]. In these conditions, both elements seemed to precipitate in a rhabdophane-type solid of formula $Nd_{1-2x}Ca_xTh_xPO_4 \cdot nH_2O$ which was proved by XRD and EPMA and correlated with the strong decrease of the normalized leaching for longer leaching time (conditions of saturation).

For (Nd,U)-britholites, uranium was easily released in the leachate ($R_L(U) = (2.0 \pm 0.4) \times 10^{-2}$ g m^{-2} d^{-1}) consequently to its oxidation and also probably to the presence of CaU_2O_{5+y} (which could appear as a less durable phase during the leaching tests) onto the surface of the pellets. However, the comparison of the $N_L(U)$ values determined on (Nd, U)-britholite samples and that of $N_L(Ca)$ obtained on Nd-britholites [11] did not seem to indicate that CaU_2O_{5+y} appears as a redhibitory phase for the immobilization of uranium in britholites.

5.2. Leaching of sintered monazite/brabantite samples

Due to high resistance of monazites and brabantites to aqueous alteration, the chemical durability of $Ca_{0.5}Th_{0.4}U_{0.1}PO_4$ and $La_{0.5}Ca_{0.25}U_{0.25}PO_4$ pellets was examined in more aggressive conditions (10^{-1} M HNO_3, $T = 363$ K). The normalized leaching $N_L(La)$, $N_L(Th)$ and $N_L(U)$ obtained at 363 K in static conditions are reported in Fig. 5. The associated normalized dissolution rates reached $R_L(U) = (1.6 \pm 0.2) \times 10^{-4}$ g m^{-2} d^{-1} for $Ca_{0.5}Th_{0.4}U_{0.1}PO_4$ and $R_L(La) = (9.7 \pm 0.4) \times 10^{-5}$ g m^{-2} d^{-1} and $R_L(U) = (1.6 \pm 0.1) \times 10^{-4}$ g m^{-2} d^{-1} for $La_{0.5}Ca_{0.25}U_{0.25}PO_4$, indicating no significant difference between monazites and brabantites during the first days of leaching.

Moreover, the nature of the dissolution seems to depend on the chemical composition of the material. Indeed, although the dissolution of $La_{0.5}Ca_{0.25}U_{0.25}PO_4$ appeared to be 'congruent' ($1.6 \leqslant R_L(U)/R_L(La) \leqslant 2.3$), it was found clearly 'incongruent' for $Ca_{0.5}Th_{0.4}U_{0.1}PO_4$ due to the quantitative precipitation of thorium during the first days of the leaching ($R_L(Th) = (2.1 \pm 1.0) \times 10^{-7}$ g m^{-2} d^{-1}; $R_L(U)/R_L(Th) \approx 760$).

More generally, all the normalized leaching rates of brabantite or monazite/brabantite samples prepared by this dry chemical route appear in good agreement with the data reported in literature for natural samples (Table 4) [19,20] and confirmed the high resistance of these ceramics to alteration even in aggressive media.

5.3. Leaching of β-TUPD pellets

For the same reasons than monazites and brabantites, the leaching of β-$Th_{3.4}U_{0.6}(PO_4)_4P_2O_7$

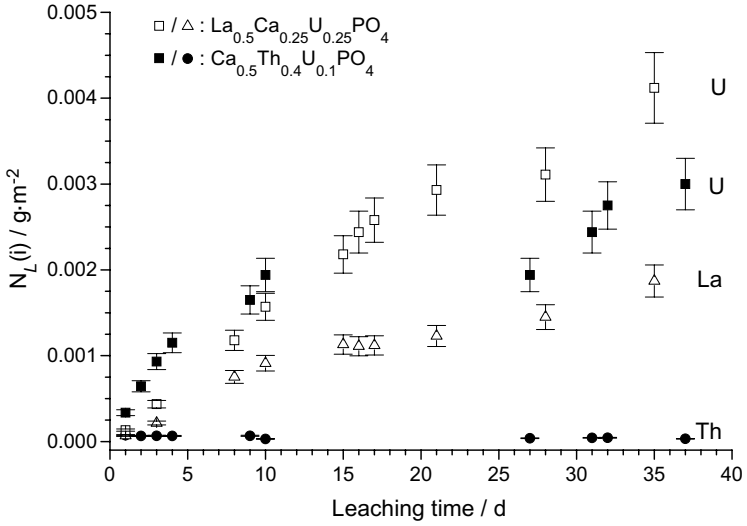

Fig. 5. Evolution of $N_L(Th)$ (●) and $N_L(U)$ (■) for leaching tests of $Ca_{0.5}Th_{0.4}U_{0.1}PO_4$ brabantite and of $N_L(U)$ (□) and $N_L(La)$ (△) for leaching tests of $La_{0.5}Ca_{0.25}U_{0.25}PO_4$ in 10^{-1} M HNO_3 ($T = 363$ K).

Table 4
Normalized dissolution rates $R_L(i)$ (g m^{-2} d^{-1}) determined for the three matrices in acidic media (HNO_3, $T = 363$ K), using static or dynamic conditions

	i	Static		Dynamic	
		10^{-1} M	10^{-4} M	10^{-1} M	10^{-4} M
$Ca_9Nd_{0.5}Th_{0.5}(PO_4)_{4.5}(SiO_4)_{1.5}F_2$	Th	ND	$(1.3 \pm 0.5) \times 10^{-4}$	ND	ND
$Ca_9Nd_{0.5}U_{0.5}(PO_4)_{4.5}(SiO_4)_{1.5}F_2$	U	ND	$(2.0 \pm 0.4) \times 10^{-2}$	ND	ND
$Ca_9Nd(PO_4)_5(SiO_4)F_2$ [11]	Ca	–	–	–	$(3.0 \pm 0.5) \times 10^{-1}$
$Ca_{0.5}Th_{0.5}PO_4$	Th	ND	$(1.7 \pm 0.3) \times 10^{-5}$	ND	$(5.7 \pm 0.2) \times 10^{-5}$
$Ca_{0.5}Th_{0.4}U_{0.1}PO_4$	U	$(1.6 \pm 0.1) \times 10^{-4}$	ND	ND	ND
$La_{0.5}Ca_{0.25}U_{0.25}PO_4$	U	$(1.6 \pm 0.1) \times 10^{-4}$	ND	ND	ND
	La	$(9.7 \pm 0.4) \times 10^{-5}$			
Natural monazite [19]	Ce	$(6.4 \pm 0.6) \times 10^{-5}$ [a]	–	$(7.5 \pm 0.8) \times 10^{-5}$ [a] $(3.8 \pm 0.4) \times 10^{-4}$ [b]	–
$GdPO_4$ [20]	Gd	$(3.8 \pm 0.8) \times 10^{-4}$	$(4.8 \pm 1.4) \times 10^{-6}$	–	–
β-TUPD ($x = 0.6$)	U	$(1.1 \pm 0.1) \times 10^{-4}$	$(5.8 \pm 0.2) \times 10^{-6}$	$(7.5 \pm 1.1) \times 10^{-5}$	$(2.9 \pm 0.3) \times 10^{-6}$
β-TUPD [15]	U	$(8.8 \pm 0.8) \times 10^{-5}$	$(2.8 \pm 0.9) \times 10^{-6}$	$(1.4 \pm 0.2) \times 10^{-4}$	$(3.3 \pm 0.1) \times 10^{-5}$ [c]

ND: Not Determined.
[a] pH = 2 and $T = 343$ K.
[b] pH = 2 and $T = 393$ K.
[c] pH = 3 and $T = 363$ K.

was examined in 10^{-1} and 10^{-4} M HNO_3. This study revealed the rapid precipitation of thorium in a phosphate-based neoformed phase (identified to $Th_2(PO_4)_2(HPO_4) \cdot H_2O$) while the uranium concentration increased progressively with the leaching time [15]. This precipitation occurred onto the surface of the pellets through the formation of an initial thin gel then its transformation into well crystallized TPHPH [21]. Consequently, the release of the elements in the leachate occurred via diffusion phenomena through these gelatinous/crystallized phases as already described for several glasses or minerals [22]. The low normalized leaching rates, determined thanks to the uranium concentration in the leachate (Table 4) confirmed the very high resistance to dissolution of β-TUPD samples prepared by this dry chemistry method.

6. Conclusions

Three phosphate-based materials loaded with tetravalent actinides (Th, U) were successfully prepared using dry chemical processes. For all the matrices, the homogeneity of the samples was significantly improved by the use of mechanical grinding and the repetition of grinding/heating cycles.

Due to differences in their redox properties, the incorporation of thorium and uranium were strongly different in the britholite structure. Indeed, while the incorporation of thorium appeared quantitative for all the compositions examined, that of uranium was limited to 3–5 wt% and associated to the formation of CaU_2O_{5+y}. On the contrary, both elements were quantitatively incorporated in single phase samples of brabantite, monazite/brabantite and β-TUPD, leading to the formation of solid solutions in all the range of composition studied.

Prior to making the leaching experiments, dense sintered pellets were prepared for each kind of material through a two-step procedure involving an uniaxial pressing at room temperature then a heat treatment ($T = 1673$ K for britholites, 1573 K for monazites/brabantites and 1523 K for β-TUPD samples). However, for the last two matrices, a reactive sintering, associated to higher final relative densities, was systematically preferred.

The study of the resistance of these three materials to aqueous alteration evaluated in aggressive media ($2.8 \quad 10^{-6}$ g m^{-2} d$^{-1} \leqslant R_L \leqslant 2.0 \quad 10^{-2}$ g m^{-2} d^{-1}) confirmed the high chemical durability of the materials considered compared to that observed for UO_2 [23] or basaltic glasses [24] even though higher normalized dissolution rates were noted for britholite samples. Finally, several neoformed phases precipitated in the back end of the initial dissolution were identified. They all appeared to be very low soluble and should contribute significantly to the delay of the release of radionuclides to the biosphere in the field of an underground repository.

References

[1] L. Boyer, J.M. Savariault, J. Carpéna, J.L. Lacout, Acta Cryst. C 54 (1998) 1057.
[2] L.A. Boatner, Rev. Mineral. Geochem. 48 (2002) 87.
[3] D. Rose, N. Jb. Miner. Mh. H 6 (1980) 247.
[4] A. Tabuteau, M. Pagès, J. Livet, C. Musikas, J. Mater. Sci. Lett. 7 (1988) 1315.
[5] R. Podor, M. Cuney, C. Nguyen Trung, Am. Mineral. 80 (1995) 1261.
[6] R. Podor, M. Cuney, Am. Mineral. 82 (1997) 765.
[7] P. Bénard, V. Brandel, N. Dacheux, S. Jaulmes, S. Launay, C. Lindecker, M. Genet, D. Louër, M. Quarton, Chem. Mater. 8 (1996) 181.
[8] N. Dacheux, R. Podor, V. Brandel, M. Genet, J. Nucl. Mater. 252 (1998) 179.
[9] N. Dacheux, A.C. Thomas, V. Brandel, M. Genet, J. Nucl. Mater. 257 (1998) 108.
[10] L. Boyer, in: 'Synthèses et caractérisations d'apatites phospho-silicatées aux terres rares: application au nucléaire, PhD-Thesis of INP Toulouse, 1998.
[11] N. Dacheux, N. Clavier, A.C. Robisson, O. Terra, F. Audubert, J.E. Lartigue, C. Guy, CR Acad. Sci. Paris 7 (2004) 1141.
[12] O. Terra, N. Dacheux, F. Audubert, C. Guy, R. Podor, Mater. Res. Soc. Symp. Proc. 802 (2004) 119.
[13] Y. Hikichi, Mineral J. 15 (1991) 268.
[14] O. Terra, in: 'Incorporation d'actinides tétravalents dans trois matrices phosphatées: britholite, monazite/brabantite et phosphate–diphosphate de thorium (β-PDT), PhD-Thesis of Université Paris-Sud-11, IPNO-T-05-03, 2005.
[15] N. Clavier, in: 'Elaboration de phosphate-diphosphate de thorium et d'uranium (β-PDTU) et de matériaux composites β-PDTU/monazite à partir de précurseurs cristallisés. Etudes du frittage et de la durabilité chimique, PhD-Thesis of Université Paris-Sud-11, IPNO-T-04-15, 2004.
[16] D. Bregiroux, S. Lucas, E. Champion, F. Audubert, D. Bernache-Assolant, J. Eur. Ceram. Soc. 26 (2006) 279.
[17] N. Clavier, N. Dacheux, P. Martinez, E. Du Fou de Kerdaniel, L. Aranda, R. Podor, Chem. Mater. 16 (2004) 3357.
[18] C. Guy, F. Audubert, J.E. Lartigue, C. Latrille, T. Advocat, C. Fillet, CR. Physique 3 (2002) 827.
[19] E.H. Oelkers, F. Poitrasson, Chem. Geol. 191 (2002) 73.
[20] O. Terra, N. Clavier, N. Dacheux, R. Podor, New J. Chem. 27 (2003) 957.
[21] A.C. Thomas, N. Dacheux, P. Le Coustumer, V. Brandel, M. Genet, J. Nucl. Mater. 281 (2000) 91.
[22] A.C. Lasaga, in: Princeton University Press (Eds), Kinetic Theory in the Earth Science, 1998.
[23] G. Heisbourg, S. Hubert, N. Dacheux, J. Ritt, J. Nucl. Mater. 321 (2003) 141.
[24] S.R. Gislason, E.H. Oelkers, Geochim. Cosmochim. Acta 67 (2003) 3817.